doi:10.1016/S0022-2836(02)01304-9 *J. Mol. Biol.* (2003) **326**, 553–568

JMB

Available online at www.sciencedirect.com

SCIENCE DIRECT®

Influence of Strand Number on Antiparallel β-Sheet Stability in Designed Three- and Four-stranded β-Sheets

Faisal A. Syud[1], Heather E. Stanger[1], Heather Schenck Mortell[1] Juan F. Espinosa[1], John D. Fisk[2], Charles G. Fry[1] and Samuel H. Gellman[1,2]*

[1]*Department of Chemistry University of Wisconsin Madison, WI 53706, USA*

[2]*Graduate Program in Biophysics University of Wisconsin Madison, WI 53706, USA*

**Corresponding author*

We describe experiments that probe whether antiparallel β-sheet secondary structure becomes more stable as the number of strands increases. Several groups, including ours, have explored this issue with pepides designed to adopt three-stranded β-sheet conformations, but the conclusions have not been consistent. In this study, we examine the effect on conformational stability of β-sheet lengthening perpendicular to the strand direction *via* analysis of designed peptides that adopt three-stranded or four-stranded antiparallel β-sheet conformations in aqueous solution. The findings reported here, along with the context provided by earlier studies, suggest that antiparallel β-sheet does, in general, become more stable when the number of strands is increased from two to three. We show that this conclusion is not influenced by the rigidity of the loop segment used to link adjacent β-strands (D-Pro-Gly *versus* Asn-Gly). We show that further extension, from three strands to four, leads to a further increase in antiparallel β-sheet stability.

Keywords: protein stability; protein design; antiparallel β-sheet; β-hairpin; NMR

Introduction

α-Helical conformations of polypeptides grow more stable as the length of the α-helix increases. This trend was demonstrated originally by comparisons among polydisperse homopolypeptides with different average molecular mass,[1] and more recently by comparisons among short, discrete peptides of varying length.[2,3] The influence of length on α-helical stability reflects a balance between the small favorable energetic effect of incorporating a residue into a pre-existing helix from a random coil state and the larger energetic penalty of starting the α-helix from a purely random coil state.[4,5] Understanding length-dependent effects and other factors that control α-helix stability is fundamental to understanding protein conformational stability at higher structural levels (tertiary, quaternary), because the α-helix is a very common substructure in folded proteins. The same is true of the β-sheet.

Does length influence the stability of β-sheet secondary structure? This question could not be addressed until it became possible to design small peptides that fold autonomously to β-sheets in aqueous solution, a relatively recent advance.[6–11] The question of length-dependence is more complex for β-sheet secondary structure than for α-helix. Two orthogonal dimensions must be considered for β-sheet, along the strands and perpendicular to the strands,[12] while only a single dimension, along the axis, is important for helices.

We have recently analyzed length-dependent effects on antiparallel β-sheet stability along the strand direction.[13] Stability was compared among a series of two-stranded β-sheets ("β-hairpins") that had an invariant core region but variable extension sequences at the termini. Lengthening the strands from five to seven residues led to increased β-hairpin stability for all extensions examined, but further lengthening to nine residues

Abbreviations used: NOE, nuclear Overhauser enhancement; NOESY, NOE spectroscopy; ROESY, rotating frame Overhauser enhancement spectroscopy; COSY, correlation spectroscopy; TOCSY, total COSY.

E-mail address of the corresponding author: gellman@chem.wisc.edu

did not lead to additional β-hairpin stability in most cases. This behavior differs from the consistent increase in α-helix stability observed upon lengthening.

Several groups have examined the effect on conformational stability of lengthening an antiparallel β-sheet perpendicular to the strand direction, by increasing the number of strands from two to three. Sharman & Searle[14] compared the extent of β-hairpin formation in the presence and in the absence of an N-terminal segment that could form a third β-strand. The three-stranded β-sheet conformation of the longer peptide (24 residues) was populated significantly in 50% (v/v) aqueous methanol but not in water. Those workers concluded that the β-hairpin was more highly populated in the context of the three-stranded β-sheet than in isolation. Independently, we designed a 20 residue, three-stranded antiparallel β-sheet that folds in water (VFITS^{D}PGKTYTEV^{D}PGOKILQ-NH_2, abbreviated ^{D}P^{D}P, (Chart 1)) to examine the same question.[12] A key element of our design was the use of D-Pro-Gly segments to form loops of two-residues between adjacent β-strands; earlier, D-Pro-Gly loops had been shown to promote β-hairpin formation in shorter peptides.[13,15–18] The D-Pro-Gly loops in ^{D}P^{D}P facilitated evaluation of the relationship between β-sheet stability and strand number because converting D-Pro to L-Pro abolishes β-hairpin formation between the adjacent strands. Therefore, comparing ^{D}P^{D}P with ^{L}P^{D}P, in which the N-terminal β-hairpin of ^{D}P^{D}P has been disrupted by L-Pro replacement, allowed us to assess the influence of the N-terminal β-hairpin on the stability of the C-terminal β-hairpin. Similarly, comparing ^{D}P^{D}P with ^{D}P^{L}P, in which the C-terminal β-hairpin of ^{D}P^{D}P has been disrupted by L-Pro replacement, allowed us to assess the influence of the C-terminal β-hairpin on the stability of the N-terminal β-hairpin. These comparisons indicated qualitatively that both the N-terminal and the C-terminal β-hairpins are populated more highly when embedded in the triple-stranded β-sheet than in isolation, i.e. that the β-sheet becomes more stable upon addition of strands.[12]

More recently, de Alba *et al*.[19] have designed a 20 residue, triple-stranded antiparallel sheet that folds in water and compared it with shorter peptides that correspond to the N-terminal β-hairpin and the C-terminal β-hairpin of this β-sheet. Those workers concluded that in neither case does the presence of the third strand lead to a significant increase in β-hairpin population, i.e. that their β-sheet does not become more stable upon addition of strands. However, the folded state populations were low for all three peptides, ca 20%, and the failure to detect length-dependent variations in β-sheet stability may have arisen from the fact that only ca 20% of the maximum effect could have been observed. Griffith-Jones & Searle[20] have designed a 24 residue peptide that folds to a three-stranded β-sheet in water and compared the stability of the C-terminal β-hairpin in the context of this β-sheet with the stability of this β-hairpin in isolation. Those workers concluded that the presence of the N-terminal strand stabilized the antiparallel β-sheet state of the two C-terminal strands by ca 0.1 kcal/mol (ΔG) at 298 K (1 cal = 4.184 J). Since this three-stranded β-sheet, like all of the peptides discussed below, is not 100% folded, the free energy increment identified by Griffiths-Jones & Searle for lengthening a β-sheet by one strand provides a lower limit for the maximum effect. Koide *et al*.[21] have shown that a single-layer antiparallel β-sheet in a natural protein can be expanded *via* strand addition without compromising the stability of the protein folding pattern. Sun & Doig[22] have developed a statistical mechanical treatment of β-sheet formation that can be used to assess length-dependent effects on conformational stability.

Here, we analyze quantitatively the influence of strand number on antiparallel β-sheet stability in aqueous solution; our approach complements and extends previous work from our group and others. We continue to employ D-Pro-Gly loops in our designs, since this segment tends to provide higher β-hairpin population than does the Asn-Gly loop used in the triple-strand designs by Searle *et al*.[14,20] or the Ser-Gly loop used in the triple-strand design by de Alba *et al*.[19] An enhanced β-hairpin population offers the prospect of observing larger thermodynamic effects exerted by distal strands. In addition, we have generated four-stranded antiparallel β-sheets that fold in water, which allow us to determine whether length-dependent effects change as a function of the number of added strands.

Results

Peptide design

In order to determine whether antiparallel β-sheet secondary structure grows more stable as strands are added, we previously relied on qualitative comparisons among NMR data for ^{D}P^{D}P and diastereomers ^{L}P^{D}P and ^{D}P^{L}P.[12] This strategy is based on the fact that D-Pro promotes β-hairpin formation strongly in surrounding residues, while L-Pro prevents β-hairpin formation. Here, we expand on the previous findings in three ways: (1) we use NMR-based population analysis to quantify the effect on β-sheet stability of additional strands; (2) we evaluate the effect of loop rigidity (D-Pro-Gly *versus* Asn-Gly) on the stabilization arising from addition of a third strand to a β-hairpin; and (3) we examine the impact of adding a fourth strand to the β-sheet. Extension to four strands is significant because we have found that length-dependent stabilization of antiparallel β-sheet along the strand direction is not monotonic.[13] It was therefore important to determine whether length-dependent stabilization of antiparallel β-sheet perpendicular to the strand direction

^{D}P^{D}P: ^{D}Pro-6, ^{D}Pro-14
^{L}P^{D}P: ^{L}Pro-6, ^{D}Pro-14
^{D}PN: ^{D}Pro-6, ^{L}Asn-14
^{L}PN: ^{L}Pro-6, ^{L}Asn-14
^{L}P^{L}P: ^{L}Pro-6, ^{L}Pro-14

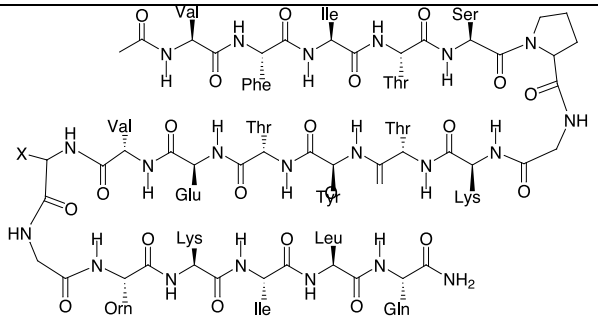

c(^{D}P)$_2$-II

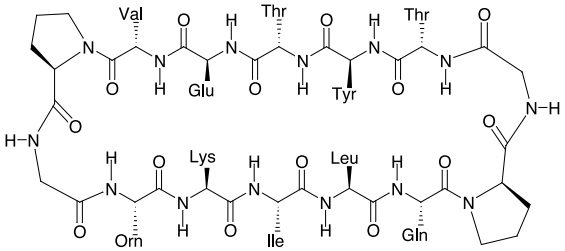

^{D}P^{D}P-II

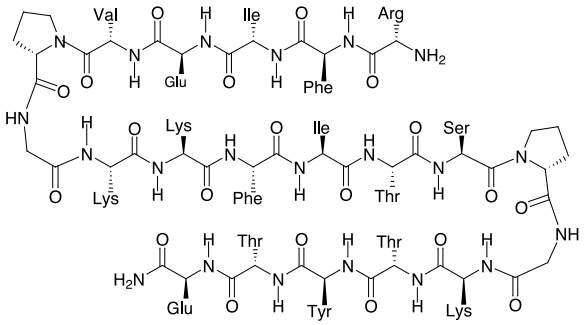

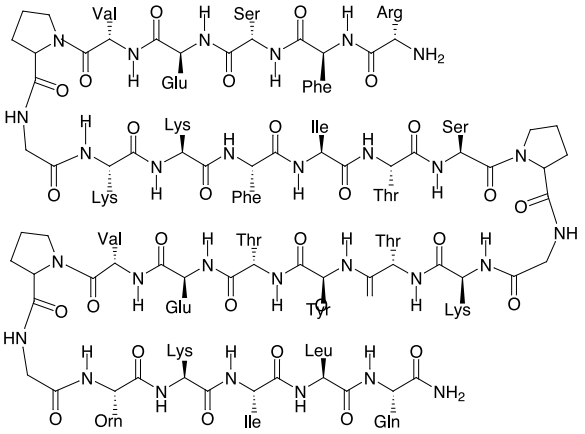

^{D}P^{D}P^{D}P: ^{D}Pro-6, ^{D}Pro-14, ^{D}Pro-22
^{L}P^{D}P^{D}P: ^{L}Pro-6, ^{D}Pro-14, ^{D}Pro-22
^{L}P^{L}P^{D}P: ^{L}Pro-6, ^{L}Pro-14, ^{D}Pro-22

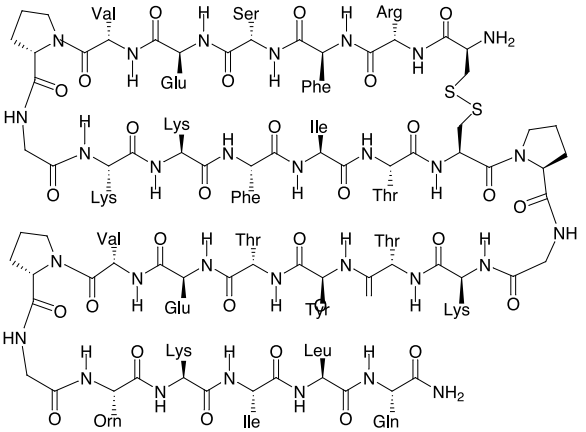

^{D}P^{D}P^{D}P-cc

Chart 1.

dissipates with increasing length, as was observed previously along the strand direction.

The design of ᴰPᴰP was based on several considerations. ᴰPᴰP contains many residues with a high propensity for β-sheet formation, e.g. those with β-branched side-chains.[23] Clustering among hydrophobic side-chains on adjacent strands is thought to stabilize β-sheets.[24–35] We tried to promote favorable interstrand contacts by pairing appropriate side-chains at non-hydrogen bonded positions that are directly across from one another in terms of the hydrogen bonded registry of the antiparallel β-sheet ("lateral pairing"). Thus, F2/T11 is a lateral non-hydrogen bonded pair in the N-terminal β-hairpin of ᴰPᴰP, and Y10/L19 is a lateral non-hydrogen bonded pair in the C-terminal β-hairpin. Side-chains paired in non-hydrogen bonded positions are oriented toward one another in the antiparallel β-sheet conformation, which provides the best opportunity for favorable hydrophobic contacts. Each hydrophobic cluster includes an aromatic side-chain in order to maximize the dispersion of ^{1}H NMR resonances. Other lateral, non-hydrogen bonded pairings were chosen because of likely favorability. Lateral non-hydrogen bonded Thr/Thr pairings appear to be favored in the antiparallel β-sheets of natural proteins,[36,37] and ᴰPᴰP has such a pairing (T4/T9). The E12/K17 pairing might lead to salt-bridge formation, depending on pH.

Peptides with a high propensity for β-sheet formation have been notorious for their tendency to aggregate.[38] We tried to discourage aggregation of ᴰPᴰP by endowing the peptide with a net positive charge. We used ornithine (O) as one of the basic residues in order to maximize ^{1}H NMR dispersion relative to the two lysine residues. Although ornithine is not a proteinogenic residue, physicochemical principles lead one to expect that the secondary structural propensity of ornithine will be very similar to those of the proteinogenic residues lysine and arginine. Indeed, we have shown that replacing ornithine with lysine in a designed β-hairpin does not cause any change in folding.[39]

ᴰPᴰP contains a second non-proteinogenic residue, D-proline. D-Pro-Gly segments are highly prone to participate in type I′ and II′ β-turn formation as residues $i+1$ and $i+2$.[40] The unusual type I′ and II′ β-turns are found commonly in the loops that connect adjacent strands of antiparallel β-sheet in proteins.[41–44] Structural analysis of several designed β-hairpins containing D-Pro-Gly loops shows that this non-proteinogenic loop generates native-like β-sheet interactions between attached strands.[17,28,45] From a design perspective, D-Pro-Gly has two advantages relative to proteinogenic sequences that have been used to induce antiparallel β-sheet secondary structure. First, D-Pro-Gly is a stronger promoter of local β-sheet structure than is Asn-Gly,[46] which is the most common proteinogenic segment in two residue β-hairpin loops.[47] Second, use of D-Pro in the loop segment facilitates design of control peptides that are critical for determining β-sheet population. Short β-sheet-forming peptides of the type discussed here are usually folded only partially. Quantifying β-sheet population can be achieved on the basis of chemical shift data, which requires control peptides that model the fully unfolded state and the fully folded state.[39] Altering the proline configuration (D → L) abolishes β-hairpin formation and generates the unfolded reference. Cyclizing a β-hairpin-forming sequence with a second D-Pro-Gly segment generates a folded reference.

ᴰPN was examined as a control to determine whether the non-proteinogenic D-Pro-Gly loop leads to unnatural conformational behavior in our β-sheet model systems. ᴰPN differs from ᴰPᴰP only at residue 14, where D-Pro in the latter is replaced by Asn in the former. Thus, the loop segment for the C-terminal β-hairpin of ᴰPN is Asn-Gly, the most common two residue β-hairpin loop observed in proteins.[43] Our quantitative analysis strategy focuses on the C-terminal β-hairpins of our β-sheet model systems; therefore, comparing results for ᴰPᴰP with results for ᴰPN will reveal whether the unnatural D-Pro-Gly loop exerts a non-native influence on the cooperative effects we are examining.

We required a four-stranded antiparallel β-sheet in order to determine whether length-dependent stabilization perpendicular to the strand direction persists upon extension from three to four strands. There is no precedent for a four-stranded β-sheet that folds autonomously in aqueous solution. (Das *et al.*[48] have reported a 26 residue peptide that adopts a four-stranded β-sheet conformation in methanol.) Our design involved appropriate positioning of D-Pro-Gly segments and proper placement of residues that could engage in favorable interstrand side-chain/side-chain contacts. The C-terminal β-hairpin of the four-stranded β-sheet was made identical with the C-terminal β-hairpin of ᴰPᴰP to facilitate quantitative analysis (*vide infra*). As discussed below, NMR-based structural analysis of ᴰPᴰP reveals clustering among the side-chains of five residues on one side of the three-stranded β-sheet, I3, S5, Y10, K17 and L19. We envisioned that a comparable cluster formed by side-chains from the first, second, and third strands (the first strand being the new strand) would promote the formation of a four-stranded β-sheet. This new cluster would occur on the opposite face of the β-sheet relative to the original I/S/Y/K/L cluster, which would then involve the second, third and fourth strands of the four-stranded sheet.

Our first step toward the design of a four-strand β-sheet was to create a three-strand β-sheet in which the first strand is new, but the second and third strands correspond to the first and second strands of ᴰPᴰP. This preliminary effort allowed us to optimize an interstrand side-chain cluster that would ultimately be complementary to the I/S/Y/K/L cluster in ᴰPᴰP. In the new design, ᴰPᴰP-II,

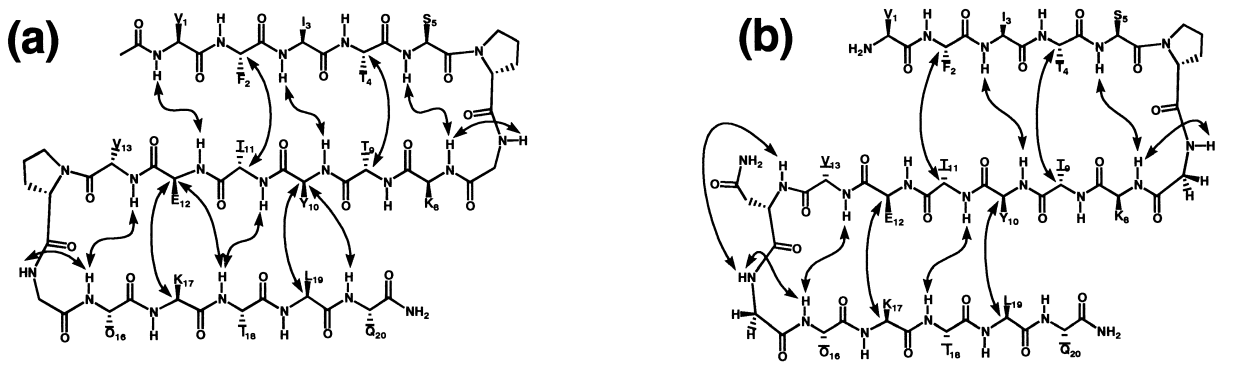

Figure 1. A summary of selected NOEs observed at 4 °C for (a) ᴰPᴰP and (b) ᴰPN in aqueous solution, pH 3.8 (uncorrected), 100 mM sodium deuterioacetate buffer. NOEs between backbone protons (NH–NH, NH–C$^{\alpha}$H and C$^{\alpha}$H–C$^{\alpha}$H) of sequentially non-adjacent residues and NOEs between protons on sequentially adjacent residues defining the turns in the β-sheet conformation are shown. Lists of proton chemical shifts and NOEs and graphical NOE summaries are in Supplementary Material.

residues I11 through V21 (C terminus) mirror residues I3 through V13 of ᴰPᴰP. Residue F2 of ᴰPᴰP has been replaced conservatively with Y10 in ᴰPᴰP-II. Residue V1 of ᴰPᴰP has been replaced with K9 of ᴰPᴰP-II to promote aqueous solubility and minimize aggregation. V5 was selected because we have observed that valine preceding D-Pro seems to promote β-turn formation, and because β-branched residues have a high propensity for β-sheet formation.[23] E4 was selected because of the possible salt-bridge with K9 (although the use of pH 3.8 for the NMR studies might preclude salt-bridge formation). I3 was selected because of a high propensity for β-sheet formation. F2 was selected in the hope that a favorable cross-strand hydrophobic interaction would occur between this side-chain and the side-chain of I11. R1 was selected to promote solubility and discourage aggregation. The side-chains of I3, V5, Y10, T17 and T19 of ᴰPᴰP-II are intended to form a stabilizing side-chain cluster in the folded state.

ᴰPᴰPᴰP represents a merger of ᴰPᴰP and ᴰPᴰP-II to generate a four-stranded design. Residues F2-Q20 of ᴰPᴰP are identical with residues F10–Q28 of ᴰPᴰPᴰP. With one exception, residues R1–K9 match one another in ᴰPᴰP-II and ᴰPᴰPᴰP (I3 in ᴰPᴰP-II is replaced with S3 in ᴰPᴰPᴰP because nuclear Overhauser enhancement (NOE) data for ᴰPᴰP-II (*vide infra*) suggested that the side-chain of I3 does not participate in the intended hydrophobic cluster). A modified four-stranded β-sheet design, ᴰPᴰPᴰP-cc, was developed. ᴰPᴰPᴰP-cc differs from ᴰPᴰPᴰP at two positions: S13 of ᴰPᴰPᴰP has been replaced by cysteine, and a second cysteine residue has been added at the N terminus. In the expected β-sheet conformation, the two cysteine residues would be juxtaposed laterally in non-hydrogen bonded positions. Disulfide formation should lock in the N-terminal β-hairpin of ᴰPᴰPᴰP-cc,[39] decreasing the number of partially folded states of ᴰPᴰPᴰP-cc relative to ᴰPᴰPᴰP, therefore enhancing any stabilizing effect exerted by the N-terminal strand, *via* the second strand, on the C-terminal β-hairpin.

Structural analysis of designed antiparallel β-sheet peptides

We previously reported 500 MHz NMR data for the designed 20-mer ᴰPᴰP showing that this peptide folds partially to a three-stranded antiparallel β-sheet conformation in aqueous solution at 24 °C.[12] This initial characterization has now been complemented by acquiring additional NMR data at 4 °C with 600 MHz and with 750 MHz spectrometers. The one-dimensional ^{1}H NMR spectrum of ᴰPᴰP displayed significantly greater resonance dispersion at 4 °C than at 24 °C. A larger number of backbone–backbone NOEs was observed at the lower temperature, including all of the C$^{\alpha}$H–C$^{\alpha}$H and NH–NH NOEs expected for the target conformation (Figure 1(a)). These data show that the β-sheet hydrogen bond registry at 4 °C is identical with that at 24 °C. Numerous NOEs were observed at 4 °C between side-chains in non-hydrogen bonded positions of each β-hairpin within ᴰPᴰP. Multiple contacts were detected for lateral pairs (F2/T11 and Y10/L19) and for pairs that are offset toward the N termini of their respective strands relative to one another (F2/T9 and Y10/K17). We refer to these latter juxtapositions as diagonal pairings. We have recently shown that diagonal side-chain contacts contribute to the stability of a designed β-hairpin closely related to the C-terminal segment of ᴰPᴰP.[45] Diagonal pairings arise from the right-handed twist that is observed commonly in β-sheets.[49] The potential significance of diagonal side-chain-side/chain contacts in β-sheet stability has received little attention to date.[45,50] A network of NOEs was observed between residues in hydrogen-bonded positions in the N-terminal β-hairpin. None of these NOEs was observed in the original analysis. Both lateral (I3/Y10) and diagonal (S5/Y10) side-chain contacts

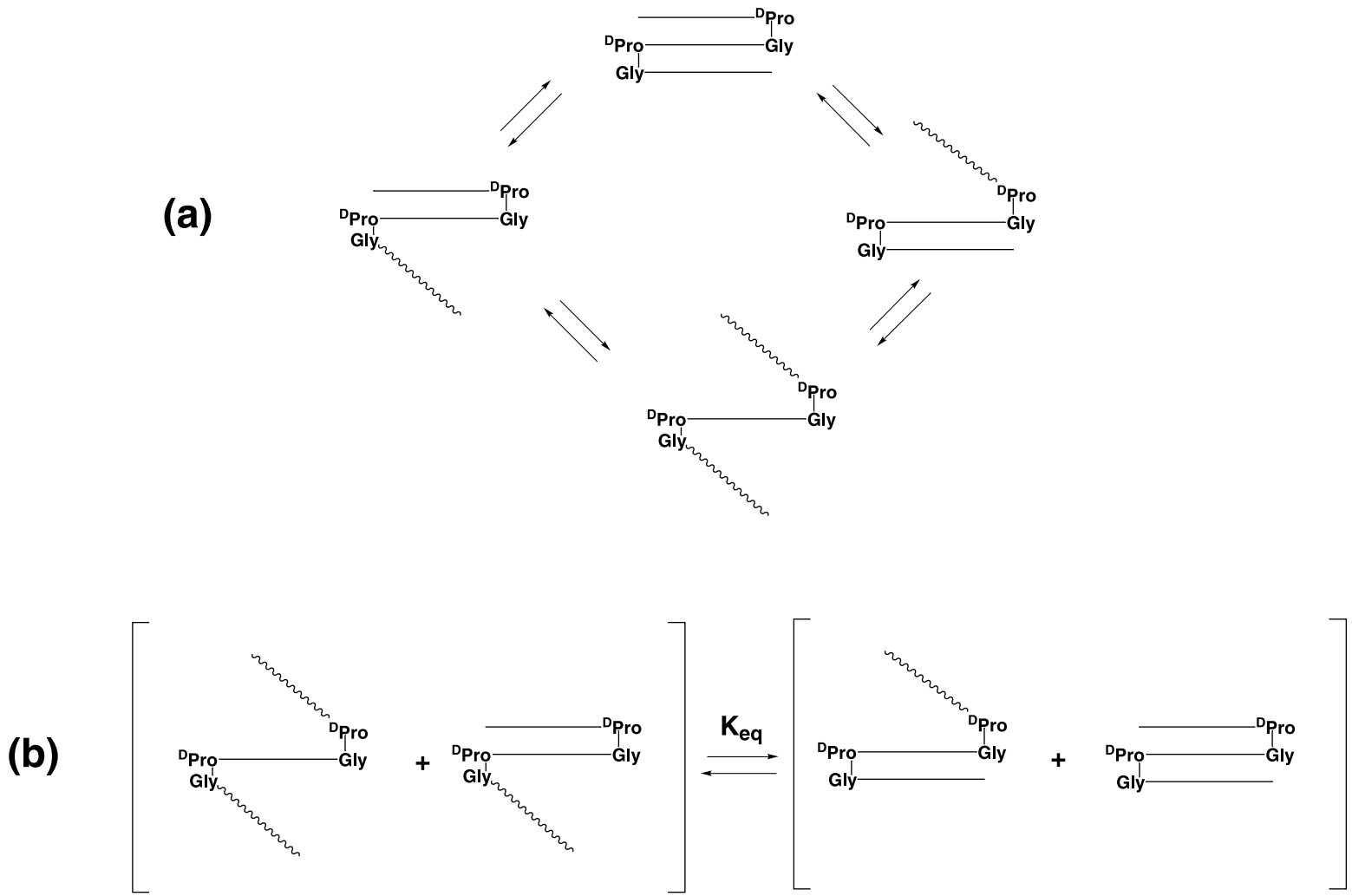

Figure 2. (a) Four-state folding model proposed for ᴰPᴰP; this model follows the analogous model proposed by Griffiths-Jones & Searle[20] for a different peptide designed to form a three-stranded β-sheet. (b) Collapse of the four-state model for ᴰPᴰP to a two-state equilibrium, C-terminal β-hairpin unfolded *versus* C-terminal β-hairpin folded, which can be monitored by chemical shift data for residues Orn16 and Ile18 in the C-terminal strand (see the text for details).

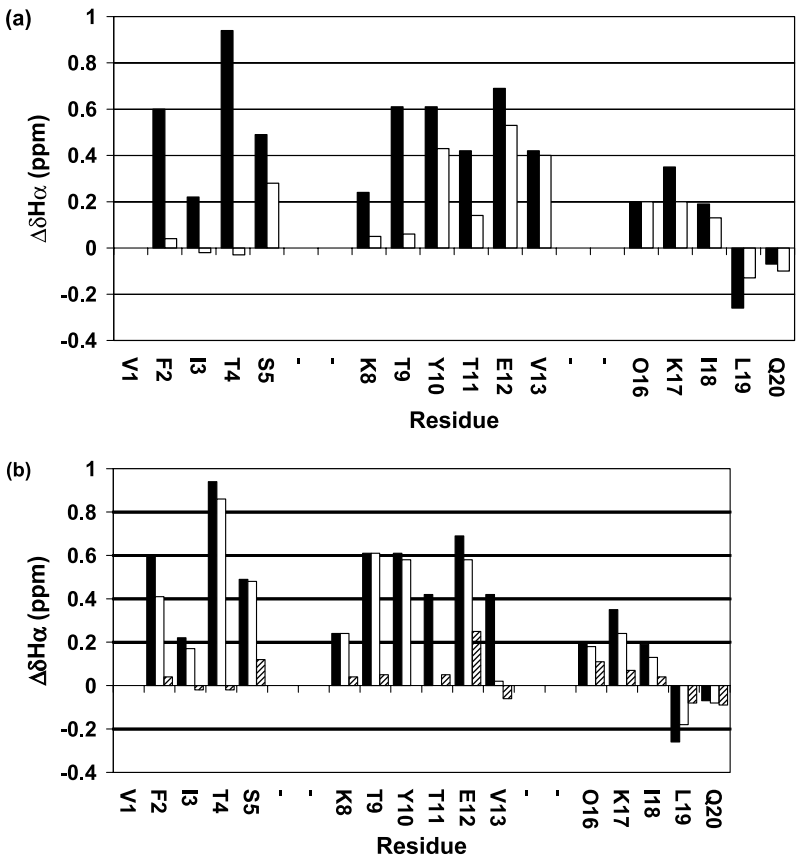

Figure 3. α-Proton chemical shift index ($\Delta\delta_{H\alpha} = \delta_{H\alpha}(obs) - \delta_{H\alpha}(random\ coil)$) for the strand residues of three-stranded designs in aqueous solution, pH 3.8 (uncorrected), 100 mM sodium deuterioacetate buffer, at 4 °C. $\delta_{H\alpha}$(random coil) values from model tetrapeptides.[54] (a) ᴰPᴰP (filled bars) and ᴸPᴰP (open bars). (b) α-Proton chemical shift index of ᴰPᴰP (filled bars) and ᴰPN (open bars), and ᴸPN (hatched bars).

were observed, but for these hydrogen bonded positions the diagonal pairing involves an offset toward the C terminus in each strand. All of these side-chain NOEs are consistent with the intended triple-stranded β-sheet conformation. No NOE inconsistent with this conformation was observed.

The large number of NOEs between residues that are not adjacent in sequence (see Supplementary Material) does not necessarily imply that ᴰPᴰP adopts a single folded conformation in aqueous solution. We have previously shown that individual β-hairpins display two-state folding behavior ("all-or-none"), but the three-stranded β-sheet probably does not. As Griffiths-Jones & Searle[20] have pointed out for a different designed three-stranded β-sheet, the conformational behavior of ᴰPᴰP is probably best described in terms of a four-state model: a fully unfolded state, a fully folded state (triple-stranded β-sheet), and partially folded states corresponding to the C-terminal β-hairpin alone and the N-terminal β-hairpin alone (Figure 2(a)). These conformational states interconvert rapidly on the NMR timescale. The NOE data indicate that no alternative folding patterns are significantly populated.

Additional evidence of β-sheet formation by ᴰPᴰP was obtained from the chemical shifts of α-protons ($\delta_{H\alpha}$) and α-carbon atoms ($\delta_{C\alpha}$), which are sensitive to secondary structure.[51–53] Residues in a β-sheet conformation generally show downfield-shifted $\delta_{H\alpha}$ relative to the unstructured or random coil state. Figure 3(a) shows $\Delta\delta_{H\alpha}$ ($= \delta_{H\alpha}(obs) - \delta_{H\alpha}(random\ coil)$) values for ᴰPᴰP at 4 °C. We follow the standard procedure of using the $\delta_{H\alpha}$ values from small unfolded peptides in the series Gly-Gly-Xxx-Ala to represent $\delta_{H\alpha}$(random coil);[54] we use the Lys value for Orn. The $\Delta\delta_{H\alpha}$ data obtained at 24 °C (not shown) display a comparable pattern but generally smaller $\Delta\delta_{H\alpha}$ values, suggesting a decrease in folded population at the higher temperature. A peptide segment is considered to be in a β-sheet conformation when three or more consecutive residues show $\Delta\delta_{H\alpha}$ values > 0.1 ppm.[53] All of the expected strand regions of ᴰPᴰP conform to this trend; deviations are seen at the two termini (presumably frayed) and L19. The negative $\Delta\delta_{H\alpha}$ value for L19 may reflect ring current effects from the nearby aromatic side-chain of Y10 in the folded state (this proximity is indicated by NOEs).

Figure 4 shows $\Delta\delta_{C\alpha}$ ($= \delta_{C\alpha}(obs) - \delta_{C\alpha}(random\ coil)$) for ᴰPᴰP at 24 °C, where the $\delta_{C\alpha}$(random coil) values are obtained from small peptides Gly-Gly-Xxx-Ala-Gly-Gly.[55] $\delta_{C\alpha}$ data show opposite trends relative to $\delta_{H\alpha}$ data: residues in a β-sheet conformation generally show upfield ^{13}C chemical shifts relative to the unstructured state.[51] The $\Delta\delta_{C\alpha}$ values for ᴰPᴰP are predominantly negative, as expected, but Y10 and L19 show positive values. The distribution of $\Delta\delta_{C\alpha}$ values for β-sheets in proteins overlaps with the distribution of $\Delta\delta_{C\alpha}$ values for α-helices, which lie downfield of the random coil

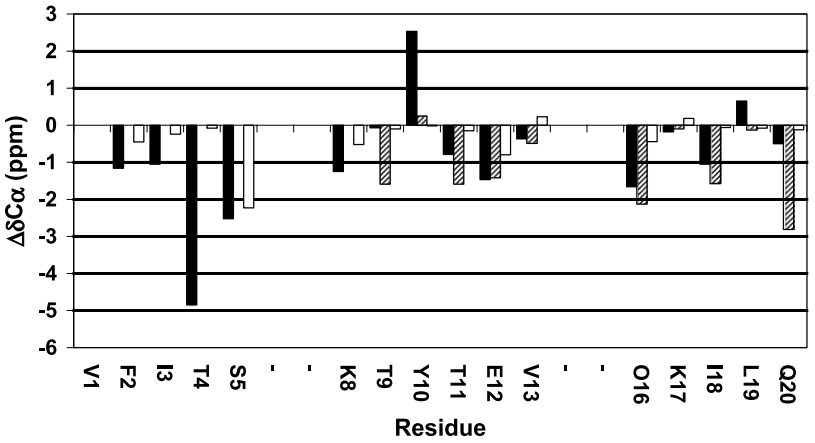

Figure 4. α-^{13}C chemical shift index ($\Delta\delta_{C\alpha} = \delta_{C\alpha}(\text{obs}) - \delta_{C\alpha}(\text{random coil})$) for the strand of ᴰPᴰP (filled bars), ᴸPᴸP (open bars) and c(ᴰP)$_2$-II (hatched bars) in aqueous solution, pH 3.8 (uncorrected), 100 mM sodium deuterioacetate buffer, at 24 °C. $\delta_{C\alpha}$(random coil) values obtained from model peptides.[55]

state;[51] therefore, observation of a few deviations from the general $\Delta\delta_{C\alpha}$ trend for ᴰPᴰP is not surprising. Our analysis of ᴰPᴰP and other systems[13] suggests that $\delta_{C\alpha}$ data do not provide a substantial improvement over $\delta_{H\alpha}$ data in terms of insight on secondary structure in designed β-sheets. Since acquisition of $\delta_{C\alpha}$ data is time-consuming at natural isotopic abundance, we rely on $\delta_{H\alpha}$ data for analysis of the remaining peptides discussed below.

NMR analysis of ᴰPN indicates that this peptide forms a three-stranded antiparallel β-sheet conformation analogous to that of ᴰPᴰP. Numerous NOEs were observed between sequentially non-adjacent residues of ᴰPN (Figure 1(b) and Supplementary Material), all of which are consistent with the expected conformation. (Chen *et al*. recently reported that the β-sheet folding pattern of ᴰPᴰP is preserved when D-Pro-14 is replaced by Asp, but not when D-Pro-6 is replaced with Asp.[56]) The number of NOEs between sequentially non-adjacent residues is smaller for ᴰPN than for ᴰPᴰP. The $\Delta\delta_{H\alpha}$ data for ᴰPN are consistent with the three-stranded β-sheet conformation throughout the sequence (Figure 3(b)), although the extent of folding appears qualitatively to be diminished relative to ᴰPᴰP.

ᴰPᴰP-II was designed as a first step toward development of a four-stranded antiparallel β-sheet model system, as described above. NMR data (not shown) indicated qualitatively that the expected three-stranded β-sheet conformation is at least partially populated in aqueous solution. The $\Delta\delta_{H\alpha}$ data for ᴰPᴰP-II revealed $\Delta\delta_{H\alpha} > +0.1$ ppm for F2-V5, K8-S13 and K16-Y18, corresponding to the N-terminal, middle and C-terminal strands, respectively, of the antiparallel β-sheet design. Numerous NOEs were observed for ᴰPᴰP-II, all of which are consistent with the three-stranded β-sheet (see Supplementary Material). NH–NH NOEs were observed for residue pairs expected to engage in interstrand hydrogen bonds with one another (I3/Y10, V5/K8, I11/Y18 and S13/K16) but not for any other sequentially non-adjacent residue pairs. In addition, side-chain/side-chain NOEs are consistent with the expected contacts. NOEs were observed between the side-chain of Y10 and the side-chains of V5, T17 and T19 (because of imperfect resolution it was impossible to distinguish between side-chain resonances of T17 and T19). Although we expected side-chain NOEs between the lateral non-hydrogen bonded pair I3/Y10, none was observed. In addition, side-chain NOEs were observed between F2 and both K9 and I11. This set of observations suggests that the N-terminal strand of ᴰPᴰP-II would be suitable for extension of ᴰPᴰP to a four-stranded β-sheet.

Qualitative NMR data indicate that the four-stranded β-sheet conformation of ᴰPᴰPᴰP is significantly populated in aqueous solution. Figure 5 shows that nearly all of the residues expected to reside in a β-strand display $\Delta\delta_{H\alpha} > +0.1$ (the three exceptions are S3, which should be directly across from F10, K8 and L27; the leucine residue analogous to L27 in ᴰPᴰP and related designs shows upfield shifts). Many NOEs were observed between residues that are not sequentially adjacent in ᴰPᴰPᴰP (see Supplementary Material), and all are consistent with the intended four-stranded β-sheet conformation. Backbone NOEs (Figure 6(a)) include most of the NH–NH NOEs expected for hydrogen bonded pairings in neighboring strands (V5/K8, K9/E20, I11/Y18, S13/K16, V21/O24 and T19/I26) and most of the $C^{\alpha}H$–$C^{\alpha}H$ NOEs expected for non-hydrogen bonded pairings in neighboring strands (E4/K9, K8/V21, F10/T19, E20/K25 and Y18/L27). In addition, each of the three glycine residues shows an NH–NH NOE with the next residue in the sequence, as expected for loop formation at each D-Pro-Gly segment. The pattern of side-chain/side-chain NOEs (see Supplementary Material) suggests clustering among three sets of side-chains: V5/F10/T17/T19, S13/Y18/K25/L27 and F2/K9/I11. In each set, the aromatic side-chain displayed multiple NOEs to each of the other residues involved, sometimes including NOEs to backbone protons. The NOE data indicate that ᴰPᴰPᴰP does not populate folded conformations other than the four-stranded β-sheet or partially folded versions thereof.

NMR data indicated that ᴰPᴰPᴰP-cc adopts a partially populated four-stranded antiparallel β-sheet conformation in aqueous solution, similar to the

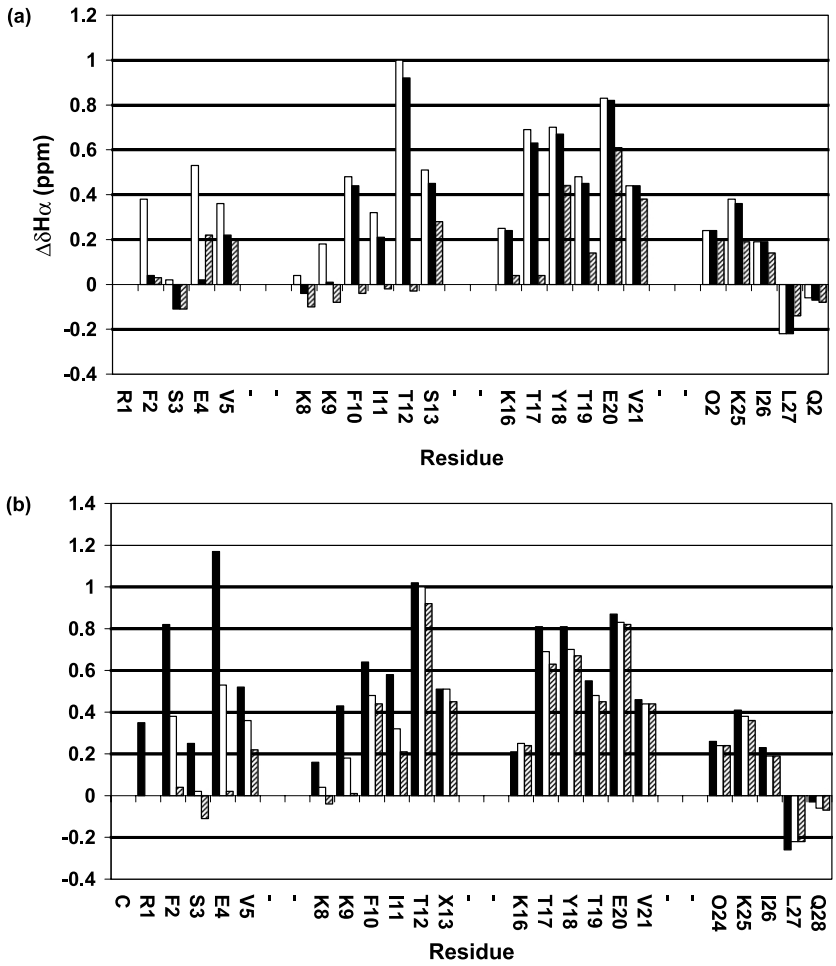

Figure 5. α-Proton chemical shift index ($\Delta\delta_{H\alpha} = \delta_{H\alpha}(obs) - \delta_{H\alpha}(random\ coil)$) for the strand residues of four-stranded designs in aqueous solution, pH 3.8 (uncorrected), 100 mM sodium deuterioacetate buffer, at 4 °C. $\delta_{H\alpha}$(random coil) values from model tetrapeptides.[54] (a) ᴰPᴰPᴰP (open bars), ᴸPᴰPᴰP (filled bars) and ᴸPᴸPᴰP (hatched bars). The value for Arg1 is not shown because the peptides are uncapped at the N termini. (b) ᴰPᴰPᴰP-cc (filled bars), ᴰPᴰPᴰP (open bars) and ᴸPᴰPᴰP (hatched bars). The value for Cys preceding Arg1 is not shown for ᴰPᴰPᴰP-cc because the peptide is uncapped at the N terminus.

conformation displayed by ᴰPᴰPᴰP. The success of the disulfide in stabilizing the N-terminal β-hairpin is indicated by $\Delta\delta_{H\alpha}$ data, which show that all residues in the N-terminal strand of ᴰPᴰPᴰP-cc have significantly larger positive values than do the analogous residues of ᴰPᴰPᴰP (Figure 5(b)). In addition, nearly all of the residues in the other three strands show larger positive values for

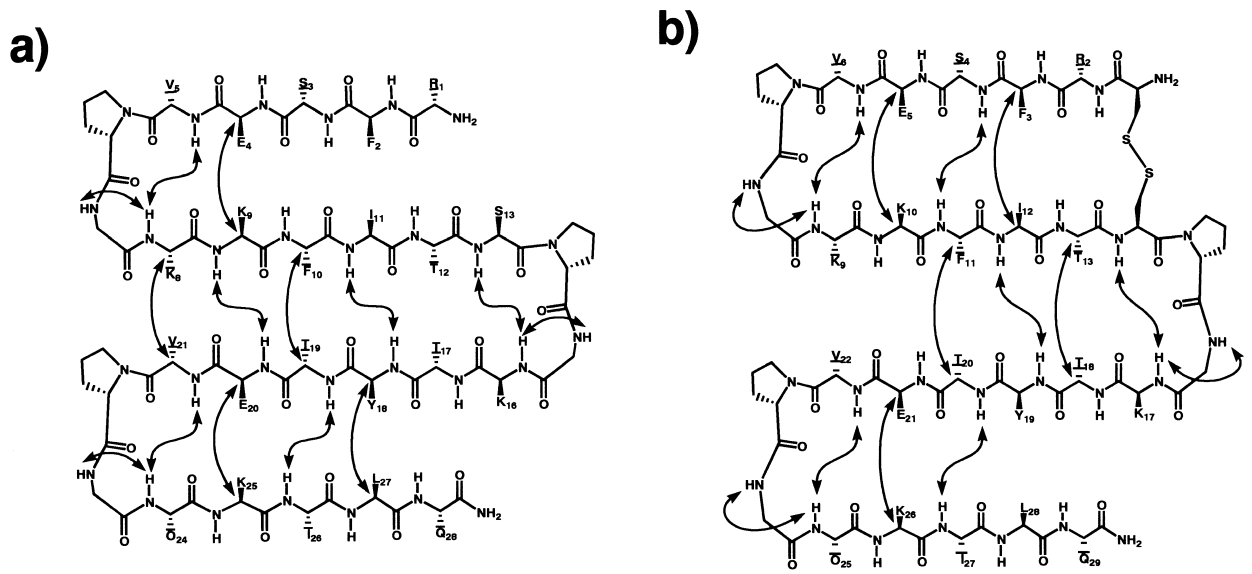

Figure 6. A summary of selected NOEs observed at 4 °C for (a) ᴰPᴰPᴰP and (b) ᴰPᴰPᴰP-cc in aqueous solution, pH 3.8 (uncorrected), 100 mM sodium deuterioacetate buffer. All NOEs between backbone protons (NH–NH and $C^{\alpha}H$–$C^{\alpha}H$) of sequentially non-adjacent residues and NH–NH NOEs between sequentially adjacent residues defining the turns in the β-sheet conformation are shown. Lists of proton chemical shifts and NOEs and graphical NOE summaries are in Supplementary Material.

ᴰPᴰPᴰP-cc than for ᴰPᴰPᴰP, although the differences between ᴰPᴰPᴰP-cc and ᴰPᴰPᴰP are smaller in the second, third and fourth strands than in the N-terminal strand. NOE data for ᴰPᴰPᴰP-cc (see Supplementary Material) are consistent with the expected folding behavior; the pattern of side-chain/side-chain NOEs is very similar to that observed for ᴰPᴰPᴰP.

β-Sheet population analysis of designed peptides

The β-sheet populations were derived from $C^{\alpha}H$ chemical shift data. $\delta_{H\alpha}$ data for short peptides like those described here represent population-weighted averages of the contributions of the unfolded and β-sheet states, which interconvert rapidly on the NMR timescale. We use L-Pro-containing peptides to model limiting $\delta_{H\alpha}$ values for the fully unfolded state, and cyclic peptides containing a second D-Pro-Gly segment to model limiting $\delta_{H\alpha}$ values for the fully folded state.[39] We have shown that this approach is successful with two designed β-hairpins,[28,45] one of which is quite similar to the C-terminal β-hairpin of ᴰPᴰP. Folding of both β-hairpins was shown to be cooperative; that is, the conformational equilibrium appeared to involve just two states, unfolded and completely folded.

In order to detect the effect of strand number on β-sheet stability, we compare C-terminal β-hairpin populations among the three-stranded and four-stranded designs described above. These population estimates are derived from NMR parameters for two residues in each C-terminal strand, Orn and Ile. This approach allows us, for example, to quantify the effect of a third strand on β-hairpin stability by focusing on $\delta_{H\alpha}$ values for residues O16 and I18 of ᴰPᴰP and ᴸPᴰP. Selection of these two residues as the "indicators" was dictated by several considerations. First, a cyclic reference peptide based on the middle and C-terminal strands of ᴰPᴰP (designated c(ᴰP)$_2$-II; Chart I) models chemical shift effects exerted by the middle strand on the C-terminal strand in the folded state and *vice versa*, but this cyclic peptide does not model the chemical shift effects exerted by the N-terminal strand on the middle strand. Therefore, $\Delta\delta_{H\alpha}$ data for residues in the middle strand of ᴰPᴰP cannot be used for quantitative studies. Second, we have previously shown that $\delta_{H\alpha}$-based population analysis of β-hairpins is successful only for hydrogen bonded residues (i.e. residues that form hydrogen bonds to the adjacent strand).[28,39,45] $\delta_{H\alpha}$ data for non-hydrogen bonded residues appear to be distorted by magnetic anisotropy effects from aromatic side-chains. Therefore, $\delta_{H\alpha}$ values for K17 and L19 cannot be used to determine the population of the C-terminal β-hairpin of ᴰPᴰP or ᴸPᴰP. Third, terminal residues like Q20 tend to be frayed.

Focusing on the population of the C-terminal β-hairpin of ᴰPᴰP allows us to collapse the four-state conformational behavior illustrated in Figure 2(a) to a two-state system, C-terminal β-hairpin unfolded *versus* C-terminal β-hairpin folded, as shown in Figure 2(b). The effect of the third strand on the population of the C-terminal β-hairpin provides quantitative insight on the enhancement of stability that arises from lengthening the sheet perpendicular to the strand direction. This strategy is extended readily to four-stranded sheets: focusing on C-terminal β-hairpin populations of ᴰPᴰPᴰP and ᴰPᴰPᴰP-**cc** allows us to collapse the multiple conformational states available to these peptides to two, C-terminal β-hairpin unfolded *versus* C-terminal β-hairpin folded, in a manner analogous to that illustrated for a three-stranded β-sheet in Figure 2(b).

The $\delta_{H\alpha}$ values for the unfolded state (δ_U) of ᴰPᴰP and related peptides were obtained from ᴸPᴸP. The $\delta_{H\alpha}$ values for the folded state of the C-terminal β-hairpin (δ_F) were obtained from cyclic peptide c(ᴰP)$_2$-II (a related cyclic peptide, designated c(ᴰP)$_2$, has been used for analysis of a β-hairpin closely related to the C-terminal β-hairpin of ᴰPᴰP.[45] NMR data confirmed that both of these reference peptides display the expected conformational behavior (see Supplementary Material). With these two sets of reference $\delta_{H\alpha}$ values in hand, one can estimate the folded population (P_β) for the C-terminal β-hairpin of ᴰPᴰP *via* equation (1) by using $\delta_{H\alpha}$ values obtained from ᴰPᴰP (δ_{obs}) and the appropriate δ_U and δ_F values. This approach can be used for population calculations based on $\delta_{C\alpha}$ values.

$$P_\beta = (\delta_{obs} - \delta_U)/(\delta_F - \delta_U) \quad (1)$$

The C-terminal β-hairpin populations deduced for O16 and I18 of ᴰPᴰP at 4 °C from $\delta_{H\alpha}$ data are reasonably consistent (83(±3)% and 75(±2)%, respectively; Table 1). Slightly lower population values were indicated by data obtained at 24 °C, 76(±3)% for O16 and 66(±3)% for I18. C-terminal

Table 1. The population of the β-sheet state at 4 °C was calculated at each indicator residue from $\delta_{\alpha H}$ data according to equation (1). $\Delta\Delta G$ was calculated for ᴰPᴰP *versus* ᴸPᴰP or ᴰPN *versus* ᴸPN in the usual way (K_{eq} for β-hairpin formation = $(\delta_{obs} - \delta_U)/(\delta_F - \delta_{obs})$; $\Delta G = -RT \ln K_{eq}$; $\Delta\Delta G = \Delta G(^{D}PX) - \Delta G(^{L}PX)$). The experimental uncertainties shown arise from the ±0.01 ppm uncertainty in $\delta_{\alpha H}$

Peptide	Residue	Population	ΔΔG (kcal/mol)
ᴰPᴰP	Orn 16	83 ± 3%	−0.42 ± 0.22
ᴸPᴰP	Orn 16	70 ± 3%	
ᴰPᴰP	Ile 18	75 ± 2%	−0.38 ± 0.13
ᴸPᴰP	Ile 18	60 ± 2%	
ᴰPN	Orn 16	63 ± 3%	−0.52 ± 0.17
ᴸPN	Orn 16	40 ± 3%	
ᴰPN	Ile 18	60 ± 2%	−0.50 ± 0.12
ᴸPN	Ile 18	37 ± 2%	

β-hairpin population at 24 °C was estimated from the $\delta_{C\alpha}$ data, 72(±1)% for O16 and 65(±1)% for I18; these results match those obtained at 24 °C from the $\delta_{H\alpha}$ data. The similarity of the populations deduced from the $\delta_{H\alpha}$ and $\delta_{C\alpha}$ data suggests that proton chemical shifts are reliable sources of population information. The good agreement between data for O16 and data for I18 is consistent with the view that C-terminal β-hairpin formation is a two-state process.

We compared ᴰPᴰP with ᴸPᴰP in order to determine the extent to which the N-terminal strand stabilizes the C-terminal β-hairpin. $\delta_{H\alpha}$-based population analysis (equation (1)) supports previous qualitative conclusions, suggesting that the C-terminal β-hairpin of ᴸPᴰP is 60–70% populated at 4 °C (Table 1). We used these population values and those calculated for ᴰPᴰP to calculate differences in stability ($\Delta\Delta G$) for the C-terminal β-hairpin embedded in a triple-stranded β-sheet (as in ᴰPᴰP) *versus* isolated C-terminal β-hairpin (as in ᴸPᴰP). This thermodynamic difference is ca 0.4 kcal/mol at both of the indicator residues (Table 1). Chemical shift data obtained at 24 °C also corresponded to a $\Delta\Delta G$ of ca 0.4 kcal/mol (data not shown). These $\Delta\Delta G$ values are lower limits on the extent of stabilization of the C-terminal β-hairpin resulting from the N-terminal strand, since the N-terminal strand is not in place 100% of the time in ᴰPᴰP.

A related comparison was carried out using the 20 residue peptides ᴰPN and ᴸPN in order to determine whether the proteinogenic Asn-Gly loop would differ from the unnatural D-Pro-Gly loop with regard to the stabilizing effect exerted by a third strand on the C-terminal β-hairpin. $\delta_{H\alpha}$-based population analysis of ᴰPN and ᴸPN was carried out for residues O16 and I18 using equation (1), with δ_U values from ᴸPᴸP and δ_F values from c(ᴰP)$_2$-II. The populations estimated for the two residues (Table 1) agree well with one another for both peptides at 4 °C: ca 62% population of the C-terminal β-hairpin for ᴰPN and ca 38% population of the C-terminal β-hairpin for ᴸPN. The difference between these two peptides suggests that the presence of the N-terminal strand stabilizes the C-terminal β-hairpin of ᴰPN by ca 0.5 kcal/mol. Thus, the $\Delta\Delta G$ increment observed for the Asn-Gly system is very similar to the increment for the D-Pro-Gly system, even though the Asn-Gly loop leads to a lower β-sheet population than the D-Pro-Gly loop. This similarity constitutes strong evidence that the non-proteinogenic D-Pro-Gly loop induces a "natural" β-sheet interaction between attached strands.

ᴰPᴰPᴰP and related peptides were used to examine the effect of a second N-terminal strand on the stability of the C-terminal β-hairpin. ᴰPᴰPᴰP was compared with diastereomers in which either D-Pro-6 was changed to L-Pro (ᴸPᴰPᴰP) or both D-Pro-6 and D-Pro-14 were changed to L-Pro (ᴸPᴸPᴰP). These alterations were expected to eliminate the N-terminal β-hairpin or eliminate both the N-terminal and middle β-hairpins, respectively. $\Delta\delta_{H\alpha}$ and NOE data confirmed qualitatively that ᴸPᴰPᴰP and ᴸPᴸPᴰP displayed the expected β-sheet secondary structure in only the segments neighboring the D-Pro-Gly loops (see Supplementary Material). Reference peptides c(ᴰP)$_2$-II and ᴸPᴸP were used to estimate $\delta_{H\alpha}$ values for the fully folded state and the fully unfolded state, respectively, of the C-terminal β-hairpin of each 28-residue peptides.

Table 2. The population of the C-terminal β-hairpin was calculated at each indicator residue from $\delta_{\alpha H}$ data according to equation (1). The experimental uncertainties shown arise from the ±0.01 ppm uncertainty in $\delta_{\alpha H}$

Peptide	Residue	Population
ᴰPᴰPᴰP	Orn 24	83 ± 3%
ᴸPᴰPᴰP	Orn 24	83 ± 3%
ᴸPᴸPᴰP	Orn 24	70 ± 3%
ᴰPᴰPᴰP-cc	Orn 24	90 ± 3%
ᴰPᴰPᴰP	Ile 26	75 ± 2%
ᴸPᴰPᴰP	Ile 26	75 ± 2%
ᴸPᴸPᴰP	Ile 26	63 ± 2%
ᴰPᴰPᴰP-cc	Ile 26	85 ± 2%

Table 2 shows C-terminal β-hairpin populations and Table 3 shows $\Delta\Delta G$ values calculated from $\delta_{H\alpha}$ data for O24 and I26 for ᴰPᴰPᴰP *versus* ᴸPᴸPᴰP and for ᴰPᴰPᴰP *versus* ᴸPᴰPᴰP. The two $\Delta\Delta G$ values for ᴰPᴰPᴰP *versus* ᴸPᴰPᴰP are zero, within experimental uncertainty. Thus, the partial presence of the N-terminal strand in the four-stranded antiparallel β-sheet conformation available to ᴰPᴰPᴰP does not seem to exert a significant effect on the stability of the C-terminal β-hairpin. A similar conclusion can be derived from the observation that the $\Delta\Delta G$ values for ᴰPᴰPᴰP *versus* ᴸPᴸPᴰP are indistinguishable from the $\Delta\Delta G$ values previously determined for ᴰPᴰP *versus* ᴸPᴰP. These results can be explained in two alternative ways. (1) Adding a fourth β-strand may not enhance the stability of the C-terminal β-hairpin, in contrast to the stabilizing effect of adding a third β-strand. (2) The fully folded state of ᴰPᴰPᴰP (all four strands in place)

Table 3. The C-terminal β-hairpin populations are shown in Table 2. $\Delta\Delta G$ was calculated for ᴰPᴰPᴰP *versus* ᴸPᴸPᴰP, etc. in the usual way ($K_{eq} = (\delta_{obs} - \delta_U)/(\delta_F - \delta_{obs})$; $\Delta G = -RT \ln K_{kq}$; $\Delta\Delta G = \Delta G(^{D}P^{D}P^{D}P) - \Delta G°$ (ᴸPᴸPᴰP), etc.). The experimental uncertainties shown arise from the ±0.01 ppm uncertainty in δ_{obs}

Peptide comparison	Residue	$\Delta\Delta G$ (kcal/mol)
ᴰPᴰPᴰP *versus* ᴸPᴸPᴰP	Orn 24	−0.42 ± 0.22
	Ile 26	−0.32 ± 0.13
ᴰPᴰPᴰP *versus* ᴸPᴰPᴰP	Orn 24	0.00 ± 0.27
	Ile 26	0.00 ± 0.15
ᴰPᴰPᴰP-cc *versus* ᴸPᴸPᴰP	Orn 24	−0.74 ± 0.35
	Ile 26	−0.67 ± 0.18

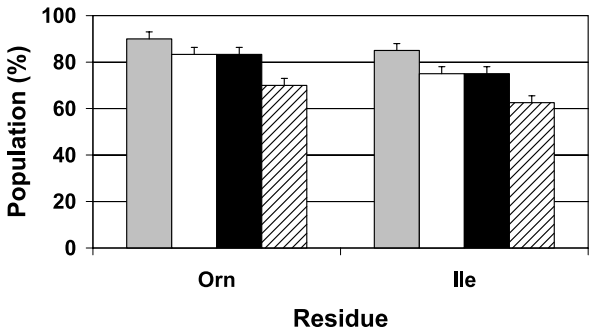

Figure 7. The C-terminal β-strand population estimated from the α-proton chemical shift data for the two indicator residues, Orn24 and Ile26, at 4 °C for peptides in the four-stranded β-sheet series: $^{D}P^{D}P^{D}P$-cc (gray bars), $^{D}P^{D}P^{D}P$ (open bars), $^{L}P^{D}P^{D}P$ (filled bars) and $^{L}P^{L}P^{D}P$ (diagonal hatched bars). The error indicated arises from the 0.01 ppm uncertainty in the measurement of $\delta_{H\alpha}$ values.

is populated to only a small extent, and the net stabilizing effect exerted by the N-terminal strand on the C-terminal β-hairpin may therefore be too small to detect.

The modified four-stranded design, $^{D}P^{D}P^{D}P$-cc, was used to distinguish between the two alternative explanations given above for the similarity in C-terminal β-hairpin stability observed for $^{D}P^{D}P^{D}P$ and $^{L}P^{D}P^{D}P$. Disulfide formation in $^{D}P^{D}P^{D}P$-cc stabilizes the N-terminal β-hairpin strongly, decreasing the number of partially folded states and therefore enhancing any stabilizing effect exerted by the N-terminal strand, *via* the second strand, on C-terminal β-hairpin formation. Figure 7 compares population values for C-terminal β-hairpins of $^{D}P^{D}P^{D}P$-cc, $^{D}P^{D}P^{D}P$, $^{L}P^{D}P^{D}P$ and $^{L}P^{L}P^{D}P$, as measured at the Orn and Ile residues in the C-terminal strand. The population deduced for $^{D}P^{D}P^{D}P$-cc appears to be higher than for the other three peptides. Table 3 shows this result in another way: $\Delta\Delta G$ for $^{D}P^{D}P^{D}P$-cc *versus* $^{L}P^{L}P^{D}P$ is significantly larger (in an absolute sense) than $\Delta\Delta G$ for $^{D}P^{D}P^{D}P$ *versus* $^{L}P^{L}P^{D}P$, although the difference is significant only for I26. Thus, this comparison suggests that cooperative stabilization of antiparallel β-sheet secondary structure can be propagated perpendicular to the strand direction through at least two strands.

Discussion

We have employed designed antiparallel β-sheets with variable numbers of strands to show that β-sheet secondary structure grows more stable as the number of strands increases. The use of D-Pro-Gly segments to link adjacent strands has facilitated this study because these dipeptide units serve as "strand-stop" signals. Thus, the positioning of D-Pro-Gly units within a designed sequence determines the length and number of the potential strand-forming segments. (Whether the strands will engage in β-sheet interactions with one another depends upon the availability of favorable interstrand side-chain/side-chain contacts.) The question of length-dependent effects on β-sheet stability would be difficult to address with β-sheets embedded in a specific tertiary structure because there is no simple way to disentangle effects arising within an embedded β-sheet from effects involving tertiary contacts between the β-sheet and the rest of the protein. Indeed, length-dependent effects on α-helix stability have been explored with autonomously folding helical peptides rather than with α-helices in proteins.[1–3]

Most short peptides that adopt specific secondary structures in water are not fully folded under accessible conditions.[5,7,9,10,57–59] Determining the folded-state population in such cases can be challenging, particularly for β-sheet models.[6] For the three-stranded and four-stranded β-sheets discussed here, the challenge is exacerbated by the population of partially folded states in which only a subset of the strands is in place.[20] We have dealt with this situation by quantifying the population of an invariant C-terminal β-hairpin as a function of the number of strands added at the N terminus (zero, one or two). Since added strands will not participate in the β-sheet conformation all the time, this strategy identifies only a lower limit for the stabilization provided by these strands to the β-hairpin under scrutiny.

In our system, adding a third strand stabilizes a two-stranded antiparallel β-sheet by a minimum of 0.4 kcal/mol. A fourth strand seems to confer a similar additional increment of stability. This increment may be compared with related values from other studies. Griffiths-Jones & Searle[20] used a different β-sheet design to assess the effect of an added strand on β-hairpin stability; a ca 0.1 kcal/mol enhancement in β-hairpin stability was observed when the third strand was at least partially in place. Given the inherent uncertainties in the population determinations of the two studies, it is not clear whether the difference between our values and that of Griffiths-Jones & Searle[20] is significant. In a complementary effort, we have examined the effect of increased length along the strand direction on β-hairpin stability.[13] Lengthening from a 12-mer to a 16-mer (i.e. lengthening each strand from five to seven residues) led to 0.2–0.3 kcal/mol stabilization, but an additional four-residue lengthening (16-mer to 20-mer) did not result in further stabilization. This non-monotonic effect of β-sheet lengthening along the strand direction contrasts with the steady increase in stability upon lengthening perpendicular to the strand direction (two *versus* three *versus* four strands). The incremental effects of length on β-sheet stability summarized here are comparable to analogous effects on α-helix stability: lengthening an alanine-rich sequence from 12 to 16 residues is expected to stabilize the α-helix by 0.65 kcal/mol.[60]

Why do added strands stabilize an existing β-sheet (in our case, a β-hairpin)? This effect probably arises, at least in part, because a β-sheet interaction between two adjacent strands conformationally preorganizes each strand for additional β-sheet interactions on the opposite side. For example, in a three-stranded β-sheet like that formed by ^{D}P^{D}P, interaction between the N-terminal strand and the central strand promotes the extended conformation of the central strand, which is necessary for interaction with the C-terminal strand. In this way, formation of one β-hairpin within the peptide lowers the entropic cost of forming the second β-hairpin.

Materials and Methods

Peptide synthesis

All linear peptides were prepared with SYNERGY 432A automated synthesizers (Applied Biosystems, Foster City, CA). Standard solid-phase Fmoc chemistry with HBTU activation and Rink Amide AM resin (Applied Biosystems, Foster City, CA) were used at a 25 μmol scale. This resin produces peptides with a primary amide group at the C termini; the N termini were not capped. Peptides were cleaved from the resin and side-chains deprotected simultaneously using trifluroacetic acid (TFA). Peptides were purified by HPLC with a C4-silica column (5 μm, 10 mm × 250 mm; Vydac, Hesperia, CA) and CH_3CN/water/TFA eluents. Homogeneity was established by analytical HPLC with C4-silica analytical column (5 μm, 4 mm × 250 mm; Vydac, Hesperia, CA) and CH_3CN/water/TFA eluents. Peptide identity was confirmed initially by matrix-assisted laser desorption time-of-flight (MALDI-TOF) mass spectroscopy, and subsequently by high-resolution ^{1}H NMR analysis.

Cyclic peptide was synthesized using an orthogonally protected glutamic acid derivative and standard solid-phase synthesis.[61] N-Fmoc-glutamic acid α-allyl ester (Novabiochem, San Diego, CA) was coupled to Rink Amide AM resin (Applied Biosystems, Foster City, CA) through the unprotected side-chain. The rest of the peptide was synthesized on resin using solid-phase methods as described above, but the final Fmoc group was not removed. The α-allyl group was removed with $Pd(PPh_3)_4$ in $CHCl_3$:AcOH:4-methylmorpholine (37:2:1, by vol.). After removal of the N-terminal Fmoc group with piperidine, cyclization was achieved using HATU. Cyclic peptides were cleaved from the resin and the side-chains deprotected with TFA; this process converted the glutamic acid to a glutamine residue. The cyclic peptide was isolated as described above.

The intramolecular disulfide bond in ^{D}P^{D}P^{D}P-cc was formed using DMSO in aqueous solution, buffered with acetic acid.[62] The linear peptide was synthesized as described. After side-chain deprotection and lyophilization, the solid form of the peptide was dissolved in an aqueous solution of 5% (v/v) acetic acid, pH adjusted to 6 by addition of NaOH or KOH. The concentration of the peptide was typically 1 mg/ml. DMSO was added to the solution such that the DMSO concentration was 15–20% (v/v). The solution was stirred open to air or with air bubbled through the solution for two days. Small amounts of water were added to maintain solution volume. The cyclic peptide was isolated as described above.

Nuclear magnetic resonance

NMR samples were prepared by dissolving lyophilized peptides in $H_2O/^{2}H_2O$ (9:1, v/v) or pure $^{2}H_2O$, 100 mM sodium deuterioacetate buffer, with pH adjusted to 3.8 with NaOH or NaO^{2}H (pH measurements were not corrected for isotope effects). This pH was chosen to minimize the amide proton exchange rate. Peptide concentrations were generally 1–2 mM. 2,2-Dimethyl-2-silapentane-5-sulfonate (DSS; Merck) was used as both an external and an internal reference.

NMR experiments were performed on Varian INOVA 500 MHz and 600 MHz spectrometers at 4 °C and 24 °C; additional NOESY and ROESY data were obtained for ^{D}P^{D}P and ^{D}P^{D}P^{D}P using a Bruker AVANCE 750 MHz spectrometer at 4 °C. All two-dimensional spectra were acquired in the phase-sensitive mode with hypercomplex phase cycling (States-Haberkorn method). Solvent suppression was achieved by 0.6–0.7 second presaturation during relaxation or a WET gradient water suppression sequence provided by Varian. Generally, a spectral window of 4500–7000 Hz was used. Standard Varian pulse sequences were used, and data were processed using Varian VNMR version 5.3 software. Sine or cosine squared window functions were generally applied after baseline correction. For chemical shift and structure assignment, COSY,[63] TOCSY,[64] NOESY[65] and ROESY[65,66] experiments were performed by collecting 2048 points in $f2$ and 400-600 points in $f1$. TOCSY experiments employed a standard MLEV-17 spin lock sequence with a spin lock field of 7–8 kHz and mixing time of 80 ms; for ROESY experiments the values were 3–3.5 kHz and 200 ms, respectively. NOESY spectra utilized mixing times of 100–200 ms. ROESY and NOESY spectra were compared to ensure absence of spin diffusion. The ^{1}H chemical shift assignment of the peptide was achieved by the sequential assignment procedure.[67] Pulsed field gradient phase-sensitive HSQC experiments were carried out using the gHSQC pulse sequence provided by Varian. A spectral window of 27,000 Hz was used for the ^{13}C dimension, which was externally referenced to DSS.

Aggregation studies

Sedimentation equilibrium experiments were carried out for ^{D}P^{D}P, ^{L}P^{D}P and ^{L}P^{L}P at 4 °C on a Beckman Optima XL-A instrument. The peptides were studied at their respective NMR sample concentrations and at lower concentrations in $H_2O/^{2}H_2O$ (9:1, v/v), 100 mM sodium deuteroacetate buffer, with pH adjusted to 3.8 with NaOH (pH measurements were not corrected for isotope effects). For each peptide, two or more revolution speeds, between 42,000 and 56,000/minute, were used. Data were analyzed using the Igor Pro program (Wavemetrics, Inc., Lake Oswego, OR). Peptides were found to be monomeric in all cases from the ideal fit of the data to a single-species model. None of the data could be fit to two-species model. However, in each case the apparent molecular mass was significantly below the expected molecular mass (by up to 30%). This behavior is attributed to the high net charge on these peptides, which leads to non-ideal behavior. Because

multistranded designs other than $^{D}P^{D}P$, $^{L}P^{D}P$ and $^{L}P^{L}P$ have an even higher net charge, variable concentration NMR analysis was used to evaluate the possibility of aggregation in these cases. Typically, the peptides were diluted by ca 100-fold from the concentration used for structural analysis and re-analyzed by one-dimensional NMR. No significant change in chemical shifts (>0.01 ppm) was observed upon dilution. At all concentrations examined for all peptides, sharp resonances, resolved at the baseline, were always observed, as would be expected from monomeric peptides.

Acknowledgements

This research was supported by the NIH (GM61238). J.F.E. was supported, in part, by a fellowship from the Ministerio de Educacion y Cultura (Spain) and the Fulbright Commission. H.E.S., H.L.S. and J.D.F. were supported, in part, by a Biophysics Training grant from NIGMS. NMR spectrometers were purchased, in part, with support from NSF and NIH. Analytical ultracentrifugation data were obtained at the NSF-supported Biophysics Instrumentation Facility at UW-Madison.

References

1. Zimm, B. H., Doty, P. & Iso, K. (1959). Determination of the parameters for helix formation in poly-γ-benzyl-L-glutamate. *Proc. Natl Acad. Sci. USA*, **45**, 1601–1607.
2. Scholtz, J. M., Qian, H., York, E. J., Stewart, J. M. & Baldwin, R. L. (1991). Parameters for helix–coil transition theory for alanine-based peptides of varying chain lengths in water. *Biopolymers*, **31**, 1463–1470.
3. Rohl, C. A., Scholtz, J. M., York, E. J., Stewart, J. M. & Baldwin, R. L. (1992). Kinetics of amide proton-exchange in helical peptides of varying chain lengths—interpretation by the Lifson–Roig equation. *Biochemistry*, **31**, 1263–1269.
4. Chakrabartty, A. & Baldwin, R. L. (1995). Stability of α-helices. *Advan. Protein Chem.* **46**, 141–176.
5. Qian, H. & Schellman, J. A. (1992). Helix-coil theories: a comparative study for finite length polypeptides. *J. Phys. Chem.* **96**, 3987–3994.
6. Gellman, S. H. (1998). Minimal model systems for β-sheet secondary structure in proteins. *Curr. Opin. Chem. Biol.* **2**, 717–724.
7. DeGrado, W. F., Summa, C. M., Pavone, V., Nastri, F. & Lombardi, A. (1999). De novo design and structural characterization of proteins and metalloproteins. *Annu. Rev. Biochem.* **68**, 779–819.
8. Koepf, E. K., Petrassi, H. M., Ratnaswamy, G., Huff, M. E., Sudol, M. & Kelly, J. W. (1999). Characterization of the structure and function of W → F WW domain variants: identification of a native unfolded protein that folds upon ligand binding. *Biochemistry*, **38**, 14338–14351.
9. Serrano, L. (2000). The relationship between sequence and structure in elementary folding units. *Advan. Protein Chem.* **53**, 49–85.
10. Searle, M. S. (2001). Peptide models of protein β-sheets: design, folding and insights in stabilising weak interactions. *J. Chem. Soc., Perkin Trans. 2*, 1011–1020.
11. Huang, X., Nakagawa, T., Tamura, A., Link, K., Koide, A. & Koide, S. (2001). Formation of the single-layer β-sheet of *Borrelia burgdorferi* OspA in the absence of the C-terminal capping globular domain. *J. Mol. Biol.* **308**, 367–375.
12. Schenck, H. L. & Gellman, S. H. (1998). Use of a designed triple-stranded antiparallel β-sheet to probe β-sheet cooperativity in aqueous solution. *J. Am. Chem. Soc.* **120**, 4869–4870.
13. Stanger, H. E., Syud, F. A., Espinosa, J. F., Giriat, I., Muir, T. & Gellman, S. H. (2001). Length-dependent stability and strand length limits in antiparallel β-sheet secondary structure. *Proc. Natl Acad. Sci. USA*, **98**, 12015–12020.
14. Sharman, G. J. & Searle, M. S. (1998). Cooperative interaction between the three strands of a designed antiparallel β-sheet. *J. Am. Chem. Soc.* **120**, 5291–5300.
15. Haque, T. S., Little, J. C. & Gellman, S. H. (1996). Stereochemical requirements for β-hairpin formation: model studies with four-residue peptides and depsipeptides. *J. Am. Chem. Soc.* **118**, 6975–6985.
16. Haque, T. S. & Gellman, S. H. (1997). Insights on β-hairpin stability in aqueous solution from peptides with enforced type I′ and type II′ β-turns. *J. Am. Chem. Soc.* **119**, 2303–2304.
17. Karle, I. L., Awasthi, S. K. & Balaram, P. (1996). A designed β-hairpin in crystals. *Proc. Natl Acad. Sci. USA*, **93**, 8189–8193.
18. Ragothama, S. R., Awasthi, S. K. & Balaram, P. (1998). β-Hairpin nucleation by Pro-Gly β-turns. Comparison of D-Pro-Gly and L-Pro-Gly sequences in an apolar octapeptide. *J. Chem. Soc., Perkin Trans. 2*, 137–143.
19. de Alba, E., Santoro, J., Rico, M. & Jiminez, M. A. (1999). *De novo* design of a monomeric three-stranded β-sheet protein. *Protein Sci.* **8**, 854–865.
20. Griffiths-Jones, S. R. & Searle, M. S. (2000). Structure, folding, and energetics of cooperative interactions between the β-strands of a *de novo* designed three-stranded antiparallel β-sheet peptide. *J. Am. Chem. Soc.* **122**, 8350–8356.
21. Koide, S., Huang, X., Link, K., Koide, A., Bu, Z. & Engelman, D. M. (2000). Design of single-layer beta-sheets without a hydrophobic core. *Nature*, **403**, 456–460.
22. Sun, J. K. & Doig, A. J. (2000). A statistical mechanical model for β-sheet formation. *J. Phys. Chem. B*, **104**, 1826–1836.
23. Muñoz, V. & Serrano, L. (1994). Intrinsic secondary structure propensities of the amino acids, using statistical Φ,Ψ matrices. Comparison with experimental scales. *Proteins: Struct. Funct. Genet.* **20**, 301–311.
24. Andersen, N. H., Dyer, R. B., Fesinmeyer, R. M., Gai, F., Liu, Z., Neidigh, J. W. & Tong, H. (1999). Effect of hexafluoroisopropanol on the thermodynamics of peptide secondary structure formation. *J. Am. Chem. Soc.* **121**, 9879–9880.
25. Carulla, N., Woodward, C. & Barany, G. (2000). Synthesis and characterization of a β-hairpin peptide that represents a "core module" of bovine pancreatic trypsin inhibitor (BPTI). *Biochemistry*, **39**, 7927–7937.
26. Cochran, A. G., Skelton, N. J. & Starovasnik, M. A. (2001). Tryptophan zippers: stable, monomeric β-hairpins. *Proc. Natl Acad. Sci. USA*, **98**, 5578–5583.

27. de Alba, E., Rico, M. & Jiménez, M. A. (1997). Cross-strand side-chain interactions *versus* turn conformation in β-hairpins. *Protein Sci.* **6**, 2548–2560.
28. Espinosa, J. F. & Gellman, S. H. (2000). A designed b-hairpin containing a natural hydrophobic cluster. *Angew. Chem., Int. Ed.* **39**, 2330–2333.
29. Espinosa, J. F., Muñoz, V. & Gellman, S. H. (2001). Interplay between hydrophobic cluster and loop propensity in β-hairpin formation. *J. Mol. Biol.* **306**, 397–402.
30. Griffiths-Jones, S. R., Maynard, A. J. & Searle, M. S. (1999). Dissecting the stability of a β-hairpin peptide that folds in water: NMR and molecular dynamics analysis of the β-turn and β-strand contributions to folding. *J. Mol. Biol.* **292**, 1051–1069.
31. Maynard, A. J., Sharman, G. J. & Searle, M. S. (1998). Origin of β-hairpin stability in solution: structural and thermodynamic analysis of the folding of a model peptide supports hydrophobic stabilization in water. *J. Am. Chem. Soc.* **120**, 1996–2007.
32. Pham, T.-N., Koide, A. & Koide, S. (1998). A stable single-layer β-sheet without a hydrophobic core. *Nature Struct. Biol.* **5**, 115–119.
33. RamÍrez-Alvarado, M., Blanco, F. J. & Serrano, L. (1996). *De novo* design and structural analysis of a model β-hairpin peptide system. *Nature Struct. Biol.* **3**, 604–612.
34. Russell, S. J. & Cochran, A. G. (2000). Designing stable β-hairpins: energetic contributions from cross-strand residues. *J. Am. Chem. Soc.* **122**, 12600–12601.
35. Searle, M. S., Griffiths-Jones, S. R. & Skinner-Smith, H. (1999). Energetics of weak interactions in a β-hairpin peptide: electrostatic and hydrophobic contributions to stability from lysine salt bridges. *J. Am. Chem. Soc.* **121**, 11615–11620.
36. Hutchinson, E. G., Sessions, R. B., Thornton, J. B. & Woolfson, D. N. (1998). Determinants of strand register in antiparallel β-sheets of proteins. *Protein Sci.* **7**, 2287–2300.
37. Wouters, M. A. & Curmi, P. M. G. (1995). An analysis of side-chain interaction and pair correlations within antiparallel β-sheets—the difference between backbone hydrogen-bonded and non-hydrogen-bonded residue pairs. *Proteins: Struct. Funct. Genet.* **22**, 119–131.
38. Nesloney, C. L. & Kelly, J. W. (1996). Progress toward understanding β-sheet structure. *Bioorg. Med. Chem.* **4**, 739–766.
39. Syud, F. A., Espinosa, J. A. & Gellman, S. H. (1999). NMR-based quantification of β-sheet populations in aqueous solution through use of reference peptides for the folded and unfolded states. *J. Am. Chem. Soc.* **121**, 11577–11578.
40. Rose, G. D., Gierasch, L. M. & Smith, J. A. (1985). Turns in peptides and proteins. *Advan. Protein Chem.* **37**, 1–109.
41. Sibanda, B. L. & Thornton, J. M. (1985). β-Hairpin families in globular proteins. *Nature*, **316**, 170–174.
42. Milner-White, E. J. & Poet, R. (1986). Four classes of β-hairpins in proteins. *Biochem. J.* **240**, 289–292.
43. Sibanda, B. L., Blundell, T. L. & Thornton, J. M. (1989). Conformation of β-hairpins in protein structures. *J. Mol. Biol.* **206**, 759–777.
44. Gunasekaran, K., Ramakrishnan, C. & Balaram, P. (1997). β-Hairpins in proteins revisited: lessons for *de novo* design. *Prot. Eng.* **10**, 1131–1141.
45. Syud, F. A., Stanger, H. E. & Gellman, S. H. (2001). Analysis of interstrand side-chain-side-chain contacts in a designed β-hairpin: significance of both lateral and diagonal interactions. *J. Am. Chem. Soc.* **123**, 8667–8677.
46. Stanger, H. E. & Gellman, S. H. (1998). Rules for antiparallel β-sheet design: D-Pro-Gly is superior to L-Asn-Gly for β-hairpin nucleation. *J. Am. Chem. Soc.* **120**, 4236–4237.
47. Hutchinson, E. G. & Thornton, J. M. (1994). A revised set of potentials for β-turn formation in proteins. *Protein Sci.* **3**, 2207–2216.
48. Das, C., Nayak, V., Raghothama, S. & Balaram, P. (2000). Synthetic protein design: construction of a four-stranded β-sheet structure and evaluation of its integrity in methanol-water systems. *J. Peptide Res.* **56**, 307–317.
49. Chothia, C. (1973). Conformation of twisted β-pleated sheets in proteins. *J. Mol. Biol.* **75**, 295–302.
50. Cootes, A. P., Curmi, P. M. G., Cunningham, R., Donnelly, C. & Torda, A. E. (1998). The dependence of amino acid pair correlations on structural environment. *Proteins: Struct. Funct. Genet.* **32**, 175–189.
51. Spera, S. & Bax, A. (1991). Empirical correlation between protein backbone conformation and Cα and Cβ ^{13}C nuclear magnetic resonance chemical shifts. *J. Am. Chem. Soc.* **113**, 5490–5492.
52. Wishart, D. S., Sykes, B. D. & Richards, F. M. (1991). Relationship between nuclear magnetic resonance chemical shift and protein secondary structure. *J. Mol. Biol.* **222**, 311–333.
53. Wishart, D. S., Sykes, B. D. & Richards, F. M. (1992). The chemical shift index: a fast and simple method for the assignment of protein secondary structure through NMR spectroscopy. *Biochemistry,* **31**, 1647–1651.
54. Bundi, A. & Wuthrich, K. (1979). 1H-NMR Parameters of the common amino acid residues measured in aqueous solutions of the linear tetrapeptides H-Gly-Gly-X-L-Ala-OH. *Biopolymers*, **18**, 285–297.
55. Wishart, D. S., Bigam, C. G., Holm, A., Hodges, R. S. & Sykes, B. D. (1995). ^{1}H, ^{13}C and ^{15}N random coil NMR chemical shifts of the common amino acids. I. Investigations of nearest-neighbor effects. *J. Biomol. NMR*, **5**, 67–81.
56. Chen, P. Y., Lin, C.-K., Lee, C.-T., Jan, H. & Chan, S. I. (2001). Effects of turn residues in directing the formation of the β-sheet and in the stability of the β-sheet. *Protein Sci.* **10**, 1794–1800.
57. Baldwin, R. L. & Rose, G. D. (1999). Is protein folding heirarchic? I. Local structure and peptide folding. *Trends Biochem. Sci.* **24**, 26–33.
58. Bolin, K. A. & Millhauser, G. L. (1999). Alpha and 3(10): the split personality of polypeptide helices. *Acc. Chem. Res.* **32**, 1027–1033.
59. Dyson, H. J. & Wright, P. E. (1991). Defining solution conformations of small linear peptides. *Annu. Rev. Biophys. Biophys. Chem.* **20**, 519–538.
60. Creighton, T. E. (1993). *Proteins*, 2nd edit., p. 185, W. H. Freeman & Co, New York.
61. Kates, S. A., Sole, N. A., Johnson, C. R., Hudson, D., Barany, G. & Albericio, F. (1993). A novel, convenient, 3-dimensional orthoganl strategy for solid-phase synthesis of cyclic-peptides. *Tetrahedron Lett.* **34**, 1549–1552.
62. Tam, J. P., Wu, C. R., Liu, W. & Zhang, J. W. (1991). Disulfide bond formation in peptides by dimethylsulfoxide—scope and limitations. *J. Am. Chem. Soc.* **113**, 6657–6662.

63. Aue, W. P., Bartholdi, E. & Ernst, R. R. (1976). Two-dimensional spectroscopy. Application to nuclear magnetic resonance. *J. Chem. Phys.* **64**, 2229–2246.
64. Bax, A. & Davis, D. G. (1985). MLEV-17 based two-dimensional homonuclear magnetism transfer spectroscopy. *J. Magn. Reson.* **65**, 355–360.
65. Jeener, J., Meier, B. H., Bachmann, P. & Ernst, R. R. (1997). Investigation of exchange processes by two dimensional NMR spectroscopy. *J. Phys. Chem.* **71**, 4546–4553.
66. Bothner-by, A. A., Stephens, R. L., Lee, J. M., Warren, C. D. & Jeanloz, R. W. (1984). Structure determination of a tetrassacharide: transient nuclear overhauser effect in the rotating frame. *J. Am. Chem. Soc.* **106**, 811–813.
67. Wüthrich, K. (1986). *NMR of Proteins and Nucleic Acids*, Wiley, New York.

Edited by P. E. Wright

(Received 8 April 2002; received in revised form 4 November 2002; accepted 5 November 2002)

Supplementary Material for this paper comprising 26 Tables and 11 Figures that provide chemical shift and NOE data is available on SCIENCE DIRECT